

# Robust Image Watermarking Based on Compressed Sensing Techniques

Hsiang-Cheh Huang

Department of Electrical Engineering  
National University of Kaohsiung  
700 University Road, Kaohsiung 811, Taiwan, R.O.C.  
hch.nuk@gmail.com

Feng-Cheng Chang<sup>1</sup>

Department of Innovative Information and Technology  
Tamkang University  
180 Linwei Road, Jiaosi, Ilan 262, Taiwan, R.O.C.  
135170@mail.tku.edu.tw

Received June 2013; revised December 2013

---

*ABSTRACT.* Compressed sensing is a newly developed topic in the field of data compression. Most of relating researches focus on compression performances or theoretical studies, and there are very few papers aiming at the integration of watermarking into compressed sensing systems. In this paper, we propose an innovative scheme that considers the copyright protection of data with compressed sensing. By carefully utilizing the relationships between compressively sensed coefficients, very few amounts of transmitted coefficients are capable of reconstructing the image to some extent. Moreover, secret information embedded beforehand can be recovered with acceptable rate in correctly extracted bits even experiencing through the lossy channels for delivery of marked image. Simulation results with our algorithm have demonstrated the effectiveness for integrating watermarking into compressive sampling systems.

**Keywords:** Compressed sensing, Watermarking, Copyright protection.

---

1. **Introduction.** Compressed sensing, also named compressive sampling, is a newly developed topic in data compression researches. Conventional approaches for sampling the signals follow the Nyquist-Shannon sampling theorem, which requires the sampling rate of more than twice the bandwidth of the signal. Therefore, it comes out an idea about how to select a sampling rate, which is smaller than the Nyquist rate, with the capability of reconstructing the original signal to some extent. Theoretical derivations may also provide some support to this viewpoint. By use of compressed sensing, such a goal of choosing a sampling rate less than the Nyquist rate may be achieved, and signals can be recovered at the decoder with the designated rate. Two principles in compressive sampling are the sparsity, which pertains to the signals of interest, and the incoherence, which relates to the sensing modality [1, 2]. They will be addressed in more detail in Sec. 2.

Because the topic of compressed sensing has emerged in the last couple of years [3, 4, 5], researches focused on the reconstruction capability of signals, with the amount of data

---

<sup>1</sup>Corresponding author.

far less than that of Shannon's theorem expected. In addition, watermarking [6, 7, 8] is an important branch in digital rights management (DRM) [9, 10, 11, 12], it would have the potential to be of great use for applying watermarking to compressively sensed media. Looking up major research databases, there are few papers aiming at compressed sensing with the application to watermarking applications that can be looked for in literature [13, 14, 15, 16, 17, 18]. In this paper, we integrate the watermarking scheme into the compressed sensing system. With the scenario for transmitting compressively sensed signals over lossy channels, which is inspired by relating researches in literature [19, 20, 21], the watermark embedded beforehand can be extracted to some degree at the receiver, meaning that the robustness can be retained, hence the copyright of original multimedia content can be protected. Besides, the watermarked image quality, or imperceptibility, with compressed sensing should be acceptable in comparison with relating standard such as JPEG2000 [22, 23].

The rest of the paper is organized as follows. In Sec. 2, we present fundamental descriptions of compressed sensing, and relating works that aim at watermarking for compressed sensing application are also addressed. Then, in Sec. 3, we present the proposed algorithm that is capable of protecting the copyright of data after compressed sensing. Robustness of proposed algorithm can be verified after transmission of protected data over lossy channels. Simulation results are demonstrated in Sec. 4, which point out the potential of integrating watermarking into the structure of compressed sensing with the proposed algorithm. Finally, we make the conclusion of this paper in Sec. 5.

**2. Background Descriptions.** In this section, we first address briefly the background descriptions and notations of compressive sampling. Then, relating works in literature and their correlation to this paper are also discussed in short. Conventional schemes and corresponding observations can be described as follows.

**2.1. Motivations.** Compressed sensing, also named compressive sampling, abbreviated as CS, aims at looking for new sampling scheme that goes against the widely acquainted Nyquist-Shannon theorem. It is composed of the sparsity principle, and the incoherence principle [1, 2].

- For the *sparsity* principle, it relates to the information rate in data compression. In compressed sensing, it is expected to be much less than the bandwidth required, and the signal can be represented by the proper basis  $\psi$ . For the signal  $x(t)$ , with the orthonormal basis  $\psi = [\psi_1, \psi_2, \dots, \psi_n]$ , it can be represented by

$$x(t) = \sum_{i=1}^n y_i \psi_i(t). \quad (1)$$

Here,  $y_i = \langle x(t), \psi_i(t) \rangle$  denotes the coefficients of  $x(t)$  in the  $i^{\text{th}}$  basis.

In practical applications, taking discrete cosine transform (DCT) or discrete wavelet transform (DWT) for example, we can reconstruct the image in the spatial domain with very few coefficients of  $y_i$  from the frequency domain because of sparsity. That is, most coefficients in the frequency domain are small, and remaining ones that are relatively large capture most of the information. If we take the  $S$  largest coefficients in magnitude for reconstruction, we obtain the reconstructed image  $x_S(t)$  by

$$x_S(t) = \sum_{i=1}^S y_i \psi_i(t). \quad (2)$$

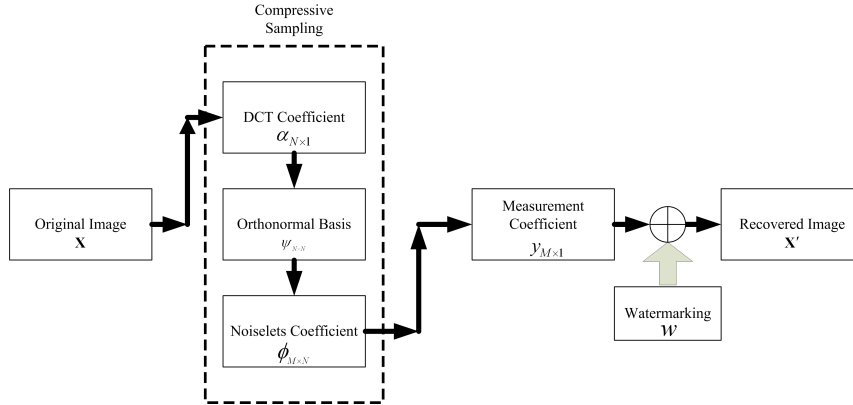


FIGURE 1. Watermark embedding with compressed sensing.

The difference between  $x(t)$  and  $x_S(t)$  should be small.

- For the *incoherence* principle, it extends the duality between time and frequency. The basis  $\varphi$ , which acts like noiselet, is employed for sensing the signal  $x(t)$ . Correlation between  $\varphi$  and  $\psi$  should lie between 1 and  $\sqrt{n}$ , where  $n$  is the number of basis in Eq. (1).

Here, we will utilize the fundamental descriptions of compressed sensing for making the integration of watermarking possible.

**2.2. Relating Topics in Literature.** There are only a few papers aiming at integrating watermarking into compressed sensing applications. We are going to make brief discussions here, and make differentiations between our proposed algorithm and those in literature [13, 14, 15, 16, 17, 18].

In [13], authors proposed an algorithm for the identification and localization of image tampering with compressed sensing. In [14], authors followed the concept of compressed sensing to conquer the intentional processing of output image with different compression ratios. In [15], authors combined the data encryption method with compressed sensing. In [16], authors apply compressed sensing to the classification of watermarked and original images. Even though the goals between these and our papers tend to provide copyright protection with compressed sensing, methods in these papers are totally different. Finally, in [17, 18], authors introduce distributed coding and the concept with the use of dictionary for integrating into compressed sensing systems.

Unlike relating topics in literature listed above, in this paper, we follow the concepts in [19, 20, 21] for developing our watermarking algorithm. At the encoder, images after compressed sensing and watermark embedding are produced, and qualities of marked images are evaluated. Then, marked images are expected to be delivered over lossy channels. At the receiver, embedded secret should be extracted to retain the copyright protection capability. Both robustness and imperceptibility, presented by bit-correct rate (BCR) and peak SNR (PSNR) respectively [12], are observed to assess the performances of proposed algorithm.

### 3. Watermarking for Compressed Sensing.

**3.1. Preliminaries.** Based on the structure of compressed sensing Fig. 1, we can integrate watermarking into the structure of compressed sensing with the following steps.

**Step 1.:** We apply DCT to the original image  $\mathbf{X}$ , and get the transform coefficient matrix  $\boldsymbol{\alpha}$ . Both have the size of  $N$ . For instance, we may turn the 2-D image with the size of  $512 \times 512$  into the 1-D array with the size of  $262144 \times 1$ .

**Step 2.:** With compressed sensing, relationship between original image and coefficient matrix can be shown with the representation matrix  $\boldsymbol{\varphi}$  in Eq. (3).

$$\mathbf{X}_{N \times 1} = \boldsymbol{\psi}_{N \times N} \boldsymbol{\alpha}_{N \times 1}. \quad (3)$$

Also, the  $M$  measurement coefficients,  $y_i$ ,  $1 \leq i \leq M$ , can be gathered to form a vector, which can be represented by Eq. (4) and Eq. (5),

$$y_i = \langle \mathbf{X}, \boldsymbol{\psi}_i \rangle. \quad (4)$$

$$\mathbf{Y}_{M \times 1} = \boldsymbol{\psi}_{M \times N} \mathbf{X}_{N \times 1}. \quad (5)$$

Here,  $\boldsymbol{\psi}$  denotes the sensing matrix. Combining Eq. (3) and Eq. (5), we can obtain

$$\mathbf{Y}_{M \times 1} = \boldsymbol{\psi}_{M \times N} \boldsymbol{\varphi}_{N \times N} \boldsymbol{\alpha}_{N \times 1}. \quad (6)$$

Because  $M$  implies the number of measurement coefficients, it should be much less than the image size  $N$ . That is,  $M \ll N$ . We choose  $K_1$  coefficients in  $\boldsymbol{\alpha}$ , and  $K_2$  coefficients in  $\boldsymbol{\varphi}$ , with the condition that  $K_1 + K_2 = M$ . We are going to perform watermark embedding with the diagram in Fig. 1.

**3.2. Watermark Embedding.** In data embedding, we group the elements in  $\mathbf{Y}$  into non-overlapping pairs. For simplicity, we suppose that  $K_1$  is an even number. The even-numbered elements in  $\mathbf{Y}$  may be changed due to data embedding in Eq. (7),

$$y'_{2m} = \begin{cases} y_{2m-1} + w, & \text{if } |y_{2m} - y_{2m-1}| < T_E; \\ y_{2m}, & \text{otherwise.} \end{cases} \quad (7)$$

We then group coefficients in Eq. (7) together to form  $\mathbf{Y}'_{M \times 1} = \{y'_1, y'_2, \dots, y'_{K_1}\}$ . Here,  $m = 1, 2, \dots, \frac{1}{2}K_1$ ,  $w$  denotes the secret bit with the value of 0 or 1, and  $T_E$  is the threshold value for data embedding. If  $T_E$  is too small, fewer secret bits can be embedded and they might be extracted in error due to lossy transmission. On the contrary, if  $T_E$  is too large, the error induced due to embedding may also increase accordingly, which would deteriorate the output image quality. Therefore, the value of  $T_E$  should be carefully chosen. After data embedding, the watermarked image  $\mathbf{X}'$  can be produced with the inverse operation calculated in Eq. (8).

$$\mathbf{X}' = \boldsymbol{\varphi}^H (\boldsymbol{\varphi} \boldsymbol{\varphi}^H)^{-1} \mathbf{Y}'. \quad (8)$$

**3.3. Data Transmission.** The watermarked image  $\mathbf{X}'$  at the output of Fig. 1 is expected to transmit over lossy channels. In our simulations, coefficients are randomly dropped, which is similar to the schemes in [19, 20, 21], and received image at the decoder is denoted by  $\mathbf{X}''$  in Fig. 2.

**3.4. Watermark Extraction.** For the extraction of embedded watermark, for the extraction of embedded watermark, compressively sensed coefficients  $\mathbf{Y}''$  need to be calculated first. Similar to Eq. (5),

$$\mathbf{Y}'' = \boldsymbol{\psi} \mathbf{X}'' \quad (9)$$

$$= \boldsymbol{\psi} \boldsymbol{\varphi} \boldsymbol{\alpha}'' \quad (10)$$

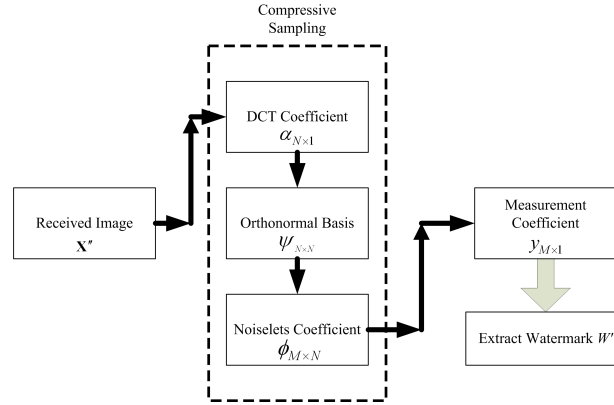


FIGURE 2. Watermark extraction with compressed sensing.

Let the extracted watermark be  $w'$ , and the one of the following conditions can be met in Eq. (11).

$$w' = \begin{cases} 0, & \text{if } |y'_{2m} - y'_{2m-1}| < T_{D1}; \\ 1, & \text{if } T_{D1} \leq |y'_{2m} - y'_{2m-1}| < T_{D2}; \\ \text{undefined,} & \text{otherwise.} \end{cases} \quad (11)$$

For practical implementations, we randomly set the value of ‘0’ or ‘1’ to the extracted watermark bit for the ‘undefined’ case in Eq. (11). Here, corresponding to the embedding procedure, in the received image, after performing compressed sensing, two neighboring coefficients are grouped as a pair. We first set the two thresholds for decoding,  $T_{D1}$  and  $T_{D2}$ , with the condition that  $0 < T_{D1} < T_{D2}$ . If the difference between the pair of coefficients is small, the extracted watermark bit is set to ‘0’. Then, when the difference grows larger, the watermark bit is set to ‘1’. Finally, if the difference is too large, no watermark bit should be extracted because such a pair might not be used for embedding, or the coefficient values might be influenced by the lossy channel.

**4. Simulation Results.** We employ two test images, **Lena** and **pepper**, with sizes of  $512 \times 512$  for conducting experiments in our simulations. With the rule of thumb that coefficients from the incoherence matrix  $\varphi$  are dozens of times more than those from the sparsity matrix  $\psi$ , we change the values of  $K_1$  and  $K_2$  accordingly. For the **Lena** image, we fix two sets of number of coefficients with  $(K_1, K_2) = (2000, 40000)$  and  $(K_1, K_2) = (1000, 20000)$ , and change the embedding threshold  $T_E$ . Here, the  $K_1$  coefficients correspond to the candidates of data embedding. For the **pepper** image, we set  $(K_1, K_2) = (2000, 21000)$  and  $(K_1, K_2) = (4096, 41000)$ , respectively.

For subjective evaluations, output image qualities can be observed from Fig. 3 for **Lena**, and Fig. 4 for **pepper**. In Fig. 3(a), we depict the reconstruction with  $K_1 = 2000$  compressively sensed coefficients, with the PSNR of 32.81 dB. In Fig. 3(b), with  $T_E = 200$ , we can embed 571 bits into the  $\frac{1}{2}K_1 = 1000$  compressively sensed pairs in Fig. 3(a), leading to the selection rate of 57.10%, and obtain the degraded quality of 29.47 dB. For making fair comparisons, we use JPEG 2000 with the same compression ratio of 131 (or 262144 : 2000) in Fig. 3(c) without watermark embedding. For viewers to evaluate subjectively, compressively sensed reconstruction in Fig. 3(a) has better quality than JPEG2000-compressed reconstruction in Fig. 3(c). Besides, the quality of watermarked reconstruction in Fig. 3(b) would be comparable to JPEG2000-compressed reconstruction without any data hiding in Fig. 3(c). For this part, we observe that compressed sensing



(a)

Recovered *Lena* with 2000 compressed sensing coefficients,  
PSNR = 32.81 dB. Image size is  $512 \times 512$ .



(b)

Recovered *Lena* with compressed sensing.  
571 bits embedded, PSNR = 29.47 dB.



(c)

JPEG2000-compressed image with the same  
compression ratio of 131 times. PSNR = 28.16 dB.

FIGURE 3. Watermarking with compressed sensing for the test image *Lena*. 2000 coefficients are selected for reconstruction of image.



(a)

Recovered pepper with  
 $(K_1, K_2) = (2000, 21000)$ ,  
 PSNR = 31.05 dB.



(b)

Watermarked pepper with  
 $(K_1, K_2) = (2000, 21000)$  and  
 $T_E = 350$ , PSNR = 30.92 dB.



(c)

Recovered pepper with  
 $(K_1, K_2) = (4096, 41000)$ ,  
 PSNR = 33.81 dB.



(d)

Watermarked pepper with  
 $(K_1, K_2) = (4096, 41000)$  and  
 $T_E = 350$ , PSNR = 33.71 dB.

FIGURE 4. Watermarking with compressed sensing for the test image **pepper**. Different numbers of coefficients are selected.

has the better performance than JPEG2000, and watermarking has the potential for the integration into compressed sensing techniques.

On the other hand, in Fig. 4, we demonstrate the compressively sensed reconstruction with or without watermark embedding for test image **pepper**. In Fig. 4(a), we set  $K_1 = 2000$ , which is the same as its counterpart in Fig. 3(a), and the output PSNR is 31.05 dB. In Fig. 4(b), we still set  $T_E = 350$  for watermark embedding into the 1000 compressively sensed pairs, and we observe slight degradation of output image quality, with the PSNR of 30.92 dB, after data embedding. In Figs. 4(c) and (d), we change  $K_1 = 4096$ , and set  $T_E = 350$ . Again, we notice slight degradation in Fig. 4(d) corresponding to its counterpart in Fig. 4(c). We also observe that the value of  $K_1$  plays an important role for reconstruction of images. The larger  $K_1$  values may lead to better quality in reconstructed

TABLE 1. Comparisons of embedding capacity and output image quality for Lena by varying embedding threshold,  $(K_1, K_2) = (2000, 40000)$ .

$T_E$	Capacity (bit)	Selection rate (%)	PSNR (dB)
0	0	0.00	32.81
200	571	57.10	29.47
250	652	65.20	28.23
350	747	74.70	26.47

image, while the compression ratio may also get decreased. With the simulations in Fig. 4, when we decrease the compression ratio from  $(\frac{262144}{2000}) = 131$  to  $(\frac{262144}{2048}) = 64$ , the quality of reconstructed image and watermarked one would get enhanced by 2.76 dB and 2.79 dB, respectively.

Finally, we depict the embedding capacity and robustness of proposed algorithm, with the test image *Lena*, in Table 1 to Table 4 for objective assessments. For the better comparisons between subjective quality and objective statistics, we may check Table 1 and Table 2 with Fig. 3(a) and Fig. 3(b) at the same time. In Table 1 and Table 3, the selection rate denotes the ratio between the numbers of secret bits to the number of pairs for embedding in Eq. (7). By increasing  $T_E$ , more capacity can be embedded, with degraded output image quality. Similar results can be observed in Table 3. However, fewer selection rate and inferior image quality for  $K_1 = 1000$  in Table 3 is presented due to the less coefficients for selection. We also observe similar trends with test image *pepper* in Fig. 4. The more compressively sensed coefficients employed lead to better output quality.

Besides, we also check robustness of extracted watermarks in Table 2 and Table 4. We can observe from Eq. (7) that the even-numbered coefficients  $y'_{2m}$  after data embedding should be close to the odd-numbered reference  $y_{2m-1}$ . Thus, we set  $T_{D1} = 1$  and  $T_{D2} = 3$  for watermark extraction in Eq. (11). With the increase in lossy rates, the bit-correct rates (BCR) decrease accordingly. BCR values are the average over twenty simulations. Comparing between the results in Table 2 and Table 4, we observe the better performance with those in Table 2. It might be because the more selection of coefficients for embedding, and the fewer possibility for erroneous extraction of output secret bits. Coefficients from noiselets, or  $K_2$ , may hardly be helpful for data extraction. Therefore, the selection of parameters, including the number of compressed sensing coefficients, the number of bit for data embedding, the thresholds for data extraction, should be carefully chosen, and be adapted with the quality requirement and the lossy rates for data transmission to obtain better results.

**5. Conclusions.** In this paper, we proposed the new application for compressed sensing with watermarking. We employ the concepts from compressed sensing, and embed

TABLE 2. Comparisons of robustness by varying lossy rates for Lena corresponding to Table 1.

$(T_{D1}, T_{D2})$	Lossy rate	BCR (%)
(1, 3)	0%	74.43
	20%	66.48
	15%	64.16
	30%	61.52

TABLE 3. Comparisons of embedding capacity and output image quality for Lena by varying embedding threshold,  $(K_1, K_2) = (1000, 20000)$ .

$T_E$	Capacity (bit)	Selection rate (%)	PSNR (dB)
0	0	0.00	30.04
200	218	43.60	28.97
250	252	50.40	28.48
350	305	61.00	27.39

the watermark into compressively sensed coefficients. Very few coefficients are necessary for image reconstruction at the encoder, and reconstructed image is delivered over lossy channels to the decoder, where data loss may be expected during delivery. With the integration of watermarking into compressed sensing techniques, we propose an effective means for retaining the ownership of this newly developed branch for data compression. The quality of watermarked reconstruction at the decoder is reasonable, while the robustness of extracted watermark can be assured. We point out this new and possible application for watermarking with compressed sensing, and further extensions and open issues may be explored subsequently based on the observations of this paper.

TABLE 4. Comparisons of robustness by varying lossy rates for Lena corresponding to Table 3.

$(T_{D1}, T_{D2})$	Lossy rate	BCR (%)
(1, 3)	0%	70.64
	20%	61.69
	15%	62.86
	30%	65.32

**Acknowledgment.** The authors would like to thank National Science Council (Taiwan, R.O.C) for supporting this paper under Grants No. NSC102-2220-E-390-002, and No. NSC100-2221-E-390-013.

#### REFERENCES

- [1] E. J. Candès, and M. B. Wakin, An introduction to compressive sampling, *IEEE Signal Processing Magazine*, vol. 25, no. 2, pp. 21-30, 2008.
- [2] J. Romberg, Imaging via compressive sampling, *IEEE Signal Processing Magazine*, vol. 25, no. 2, pp. 14-20, 2008.
- [3] T. T. Do, T. D. Tran, and L. Gan, Fast compressive sampling with structurally random matrices, *Proc. of IEEE International Conference on Acoustics, Speech and Signal Processing*, pp. 3369-3372, 2008.
- [4] G. Mateos, and G. B. Giannakis, Robust nonparametric regression via sparsity control with application to load curve data cleansing, *IEEE Trans. Signal Processing*, vol. 60, no. 4, pp. 1571-1584, 2012.
- [5] C. Deng, W. Lin, B. S. Lee, and C. T. Lau, Robust image coding based upon compressive sensing, *IEEE Trans. Multimedia*, vol. 14, no. 2, pp. 278-290, 2012.
- [6] L. Li, S. Li, A. Abraham, and J. S. Pan, Geometrically invariant image watermarking using Polar Harmonic Transforms, *Journal of Information Sciences*, vol. 199, pp. 1-19, Sep. 2012.
- [7] L. Li, J. S. Pan, and X. Yuan, High capacity watermark embedding based on invariant regions of visual saliency, *IEICE Trans. Fundamentals of Electronics, Communications and Computer Sciences*, vol. 94, no. 2, pp. 889-893, 2011.
- [8] H. C. Huang, and Y. H. Chen, Application of genetic-based wavelet packet watermarking for trusted communication, *Journal of International Information Institute*, vol. 16, no. 1, pp. 295-306, 2013.
- [9] A. Benhocine, L. Laouamer, L. Nana, and A. C. Pascu, New images watermarking scheme based on singular value decomposition, *Journal of Information Hiding and Multimedia Signal Processing*, vol. 4, no. 1, pp. 9-18, 2013.
- [10] H. C. Huang, and W. C. Fang, Metadata-based image watermarking for copyright protection, *Journal of Simulation Modelling Practice and Theory*, vol. 18, no. 4, pp. 436-445, 2010.
- [11] S. W. Weng, S. C. Chu, N. Cai, and R. X. Zhan, Invariability of mean value based reversible watermarking, *Journal of Information Hiding and Multimedia Signal Processing*, vol. 4, no. 2, pp. 90-98, 2013.
- [12] H. C. Huang, Y. H. Chen, and A. Abraham, Optimized watermarking using swarm-based bacterial foraging, *Journal of Information Hiding and Multimedia Signal Processing*, vol. 1, no. 1, pp. 51-58, 2010.

- [13] G. Valenzise, M. Tagliasacchi, S. Tubaro, G. Cancelli, and M. Barni, A compressive-sensing based watermarking scheme for sparse image tampering identification, *Proc. of the 16th IEEE international conference on Image processing*, pp. 1257-1260, 2009.
- [14] M. A. Sheikh, and R. G. Baraniuk, Blind error-free detection of transform-domain watermarks, *IEEE International Conference on Image Processing*, pp. 453-456, 2007.
- [15] R. Huang, and K. Sakurai, A robust and compression-combined digital image encryption method based on compressive sensing, *Proc. of the 7th International Conference on Intelligent Information Hiding and Multimedia Signal Processing*, pp. 105-108, 2011.
- [16] C. Patsakis, and N. Aroukatos, LSB and DCT steganographic detection using compressive sensing, *Journal of Information Hiding and Multimedia Signal Processing*, vol. 5, no. 1, pp. 20-32, 2014.
- [17] X. Zhang, A. Wang, B. Zeng, and L. Liu, Adaptive distributed compressed video sensing, *Journal of Information Hiding and Multimedia Signal Processing*, vol. 5, no. 1, pp. 121-132, 2014.
- [18] X. Sun, W. Song, Y. Lvi, and L. Tang, A new compressed sensing algorithm design based on wavelet frame and dictionary, *Journal of Information Hiding and Multimedia Signal Processing*, vol. 5, no. 2, pp. 283-294, 2014.
- [19] J. S. Pan, M. T. Sung, H. C. Huang, and B. Y. Liao, Robust VQ-based digital watermarking for the memoryless binary symmetric channel, *IEICE Trans. Fundamentals of Electronics, Communications and Computer Sciences*, vol. E-87A, pp. 1839-1841, 2004.
- [20] J. S. Pan, Y. C. Hsin, H. C. Huang, and K. C. Huang, Robust image watermarking based on multiple description vector quantisation, *Journal of Electronics Letters*, vol. 40, no. 22, pp. 1409-1410, 2004.
- [21] H. C. Huang, S. C. Chu, J. S. Pan, C. Y. Huang, and B. Y. Liao, Tabu search based multi-watermarks embedding algorithm with multiple description coding, *Journal of Information Sciences*, vol. 181, no. 16, pp. 3379-3396, 2011.
- [22] P. Schelkens, A. Skodras, and T. Ebrahimi, *The JPEG2000 suite*, Wiley, USA 2009.
- [23] Y. H. Chen and H. C. Huang, A progressive image watermarking scheme for JPEG 2000, *Proc. of the 8th International Conference on Intelligent Information Hiding and Multimedia Signal Processing*, pp. 230-233, 2012.